NASA Technical Memorandum 100192

Dynamic Delamination Buckling in Composite Laminates Under Impact Loading: Computational Simulation

Joseph E. Grady, Christos C. Chamis, and Robert A. Aiello
Lewis Research Center
Cleveland, Ohio

Prepared for the
Second Symposium on Composite Materials: Fatigue and Fracture
sponsored by the American Society for Testing and Materials
Cincinnati, Ohio, April 26-30, 1987

NASA

DYNAMIC DELAMINATION BUCKLING IN COMPOSITE LAMINATES UNDER IMPACT LOADING: COMPUTATIONAL SIMULATION

Joseph E. Grady, Christos C. Chamis, and Robert A. Aiello
National Aeronautics and Space Administration
Lewis Research Center
Cleveland, Ohio 44135

SUMMARY

A unique dynamic delamination buckling and delamination propagation analysis capability has been developed and incorporated into a finite element computer program. This capability consists of: (1) a modification of the direct time integration solution sequence which provides a new analysis algorithm that can be used to predict delamination buckling in a laminate subjected to dynamic loading, and (2) a new method of modeling the composite laminate using plate bending elements and multipoint constraints. This computer program is used to predict both impact induced buckling in composite laminates with initial delaminations and the strain energy release rate due to extension of the delamination. It is shown that delaminations near the outer surface of a laminate are susceptible to local buckling and buckling-induced delamination propagation when the laminate is subjected to transverse impact loading. The capability now exists to predict the time at which the onset of dynamic delamination buckling occurs, the dynamic buckling mode shape, and the dynamic delamination strain energy release rate.

INTRODUCTION

Composite laminates are subject to delamination, which causes a loss of both stiffness and strength. Delamination is generally induced by static, dynamic, or fatigue loading. Delaminated sublaminates are particularly susceptible to dynamic local buckling when subjected to impact loading. The prediction of impact-induced dynamic delamination buckling is necessary for evaluating the durability of many composite structures and is, therefore, the topic of this paper.

The delamination buckling phenomenon has been observed experimentally under static and fatigue loading conditions (refs. 1 to 4), and several analytical methods have been proposed to model this damage mechanism. One-dimensional beam models and fracture mechanics approaches (refs. 5 and 6) have been used to gauge the stability of delaminations in compressively loaded laminates. Finite element approaches (refs. 7 and 8) are often used for these analysis.

In the course of earlier research, experimental observations of dynamic delamination buckling in transversely impacted laminates were reported (ref. 9) based on high-speed photography of the delamination buckling sequence. This work motivated the present development of a finite element analysis technique to predict the occurrence of impact-induced dynamic buckling in laminates with delaminations. It has been shown (refs. 9 and 10) that the mechanism causing

extension of a delamination depends on the location of that delamination within the impacted laminate. A delamination along the midplane of a symmetrical laminate will initially extend in a predominantly Mode II fashion. Delaminations off the midplane (closer to the outer surface) of a laminate, however, are susceptible to buckling caused by compressive stress in the delaminated region.

This local buckling may then induce a Mode I dominated extension of the delamination. In the latter case, the ability to predict the onset of dynamic delamination buckling is essential to determine if extension of the delamination will occur when the laminate is subjected to a given impact load. The objectives of this paper are: (1) to outline the computational procedure for dynamic delamination buckling and delamination propagation, and (2) to present typical results of this procedure for a delaminated composite laminate under impact loading.

DYNAMIC BUCKLING ANALYSIS

To perform the dynamic delamination buckling analysis, the direct time integration solution sequence in the finite element program is altered so that a linear buckling analysis is performed at each time step. The buckling analysis requires solutions of the eigenvalue problem:

$$\left[[K] + \lambda[K_\sigma]\right] \{\phi\} = 0 \qquad (1)$$

where

[K] is the structural stiffness matrix

$[K_\sigma]$ is the stress stiffness matrix

The formulation of these matrices for the NASTRAN Quad-4 plate element used here is given in reference 11.

Each scalar eigenvalue satisfying equation (1) physically represents the nondimensional ratio

$$\lambda = \frac{\sigma A}{P_*}$$

where σ is the time-dependent compressive longitudinal stress in the delaminated sublaminate, A is the cross-sectional area of the sublaminate, and P_* is the critical compressive load that will cause buckling of the sublaminate. When an eigenvalue reaches the critical value of unity ($\sigma A = P_*$), buckling in that mode occurs. The eigenvectors $\{\phi\}$ associated with each eigenvalue are the corresponding dynamic buckling mode shapes. Figure 1 is a flowchart of the modified solution procedure. This altered finite element solution procedure was implemented in Version 65A of MSC/NASTRAN using NASTRAN DMAP alters. The complete modification is shown in the NASTRAN DMAP Alter sequence in Appendix A.

FINITE ELEMENT MODELING PROCEDURE

Figure 2 is a schematic diagram of the beam-like unidirectional $[0]_{10s}$ graphite/epoxy laminate with an initial 5.08 cm (2.0 in.)* long delamination through the width and located halfway between the beam midplane and outer surface. The finite element model of this specimen consisted of a uniform mesh of 800 four-node isoparametric plate-bending elements (QUAD-4 elements in MSC/NASTRAN) arranged as shown schematically in figure 3. Four elements were used in the thickness direction, so each finite element represents 5 plies of the 20-ply unidirectional laminate. Although a relatively fine, uniform finite element mesh was used for simplicity in this example, a somewhat coarser mesh is allowable in regions where high stress gradients are not anticipated. To make the most efficient use of computer time, larger elements may be used in regions remote from the delamination without sacrificing any accuracy.

The allowable displacements of adjoining nodal points in the thickness direction were constrained, using multipoint constraint equation sets, so as to satisfy simple beam bending assumptions away from the delaminated region and in each of the sublaminates in the delaminated region. These assumptions are:

(1) Plane sections remain plane
(2) No strain in the transverse (Z) direction

The first constraint set restricts neighboring nodal points in the thickness direction to deform along a straight line over the cross section (shear deformation is neglected) while the beam midplane remains unstrained. The second constraint set prevents neighboring plies from penetrating into each other. These constraints are relaxed near the delaminated region so that the displacements of the nodal points defining the delamination are allowed to deform as the solution dictates, independent of the deformation of the neighboring plies. This allows the delaminated region to separate from the main laminate when a local compression occurs in that area, as shown in figure 4. The constraints used here are shown schematically in figure 5.

Typical unidirectional graphite/epoxy material constants were used in the finite element analysis; $E_1 = 134.4$ GPa (19.5×10^6 psi), $E_2 = 10.3$ GPa (1.5×10^6 psi), $G_{12} = 5.0$ GPa (0.725×10^6 psi), $\upsilon_{12} = \upsilon_{13} = \upsilon_{23} = 0.3$, and $\rho = 1580$ kg/m^3 (1.49×10^{-4} lb-s^2/in.^{4}). The 1-direction (longitudinal) is assumed to be aligned with the fibers, while the 2-direction (transverse) is perpendicular to the fibers and in the plane of the laminate. The 3-direction is perpendicular to the plane of the laminate. A representative triangular loading, shown in figure 2, is applied at the midpoint of the laminate to simulate transverse impact. Both ends of the laminate are assumed to be rigidly supported.

RESULTS AND DISCUSSION

Figures 6 and 7 show the midplane displacement and bending stress response of a $[0]_{10s}$ laminate without an initial delamination. It is apparent

*Original measurements were in inches.

that the boundaries (clamped ends) have no effect on the structural response before 250 μs for the specimen geometry studied. Furthermore, if a delamination exists in the region of high compressive flexural stress 5 to 8 cm (2 to 3 in.) from the impact point, local buckling of the sublaminate region may occur in the 150 to 250 μs interval.

A 5.08 cm (2.0 in.) long, off-midplane delamination is now introduced into the finite element model as shown in figure 4 by removing the constraints described between two adjacent plies in the region from $x = 5.08$ to $x = 10.16$ cm ($x = 2$ to $x = 4$ in.) from the impact point. The calculated dynamic displacement of the partially delaminated specimen under the same loading is shown in figure 8. Only the displacement of the right half of the laminate is shown, in order to more clearly highlight the opening profile of the delamination. Results of the simultaneous dynamic buckling analysis are shown in figure 9. The lowest eigenvalue reaches the critical value of 1.0 approximately 190 μs after impact, for the impact loading condition shown in figure 2. These results indicate that a first-mode buckling is likely to occur approximately 190 μs after the impact event begins, for the given loading conditions. The buckling may then induce extension of the delamination in one direction or the other.

Progressive extension of the initial delamination is modeled by removing the constraints between neighboring plies at the appropriate nodal points. This approach is used here to perform finite element analyses of impacted laminates with successively increasing delamination crack lengths. A simple technique is then used to calculate the variation of the dynamic strain energy release rate with time during the interval on which the impact load acts. Using the applied force, $F(t)$, and the displacement, $y(t)$, at the point of impact, the amount of energy stored in the structure at any time t is

$$W(t) = \int_0^{y(t)} F(\xi)\, d\xi$$

This calculation is performed for several successive increments in crack length, each increment being equal to one element length in the finite element model.

Defining

$$G_T = \left.\frac{\partial W}{\partial A}\right|_{a=a_o} = \frac{W(a_o + \Delta a) - W(a_o)}{\Delta A}$$

as the total strain energy release rate;

where

a = crack length

A = crack area

the variation of strain energy release rate with time at each tip of the 5.08 cm (2.0 in.) long initial delamination is shown in figure 10. This indicates that, in the absence of flexural wave reflections from the boundaries,

the delamination will initially extend toward the point of impact. Variation of the energy release rate as the initial crack length is extended toward the point of impact is shown in figure 11. The apparent trend for the magnitude of the energy release rate to decrease as the crack length is increased indicates that the available strain energy for delamination extension will decrease monotonically, leading to stable delamination growth and eventual arrest.

RELEVANCE TO EXPERIMENTAL OBSERVATIONS

The dynamic delamination buckling analysis procedure presented here was used to predict the observed delamination buckling of the cantilevered specimen shown schematically in figure 12, which was tested as described in reference 9. The impact force history and material properties used in the analysis are from reference 9. Figure 12 shows the calculated variation of the lowest eigenvalue with time, and the associated buckling mode shape. The eigenvalue behavior indicates a first-mode delamination buckling approximately 150 μs from the beginning of impact. This is in reasonable agreement with the photographic data in reference 9, which shows delamination buckling and initial crack extension occurring between 2 to 3 frames (125 to 187.5 μs) from the beginning of impact. Further experimental investigation is currently being conducted to provide additional verification and will be reported in the near future.

POSSIBLE EXTENSIONS

The methods described here can be extended in a straightforward manner to analyze the problem of dynamic buckling and extension of an arbitrarily shaped embedded delamination in a laminated plate. This problem has been analyzed previously under static loading conditions (refs. 7 and 12). The analysis procedure for the plate will be similar to that used for the beam-like laminate geometry used here, although the physical meaning of the buckling eigenvalue will be slightly modified due to the more complex stress field. Further application of this crack-extension modeling procedure to analyze the growth of both transply cracks and edge cracks in composite laminates is possible. Embodying these extensions into the computational procedure will make it possible to assess damage tolerance and structural fracture in composites subjected to impact loads.

CONCLUSIONS

A dynamic delamination buckling analysis procedure for composite laminates with delaminations has been developed and incorporated into a finite element computer program. This algorithm enables the modified finite element program to predict: (1) the time at which delamination buckling occurs, and (2) the dynamic buckling mode shape. Preliminary experimental verification has supported the validity of the analysis.

The procedure used here to model the composite laminate allows progressive extension of the delamination to be simulated by removing the appropriate constraints between displacements at neighboring nodal points. This slightly increases the total number of degrees of freedom to be solved for in the finite

element analysis, while keeping the number of elements and the element mesh constant as the crack extends. This procedure greatly simplifies the simulation of progressive crack extension. It was used to calculate the dynamic delamination strain energy release rate for a composite laminate under impact loading.

Results obtained show that: (1) delaminations near the outer surface of a laminate that is subjected to transverse impact loading are susceptible to dynamic buckling and buckling-induced propagation, and (2) in the absence of boundary effects, transverse impact at a point near a delamination will cause the delamination to propagate toward the point of impact, with little or no extension in the opposite direction.

Further application of this procedure to the problem of buckling and propagation of an embedded delamination in a laminated plate is possible. In addition, similar techniques can be used to model different flaw types such as transply cracks and edge cracks. With these modifications it would be possible to computationally assess the damage tolerance of composite structures with initial or induced defects when subjected to impact loading.

REFERENCES

1. Gillespie, J.W., and Pipes, R.B., Composite Structures, Vol. 2, No. 1, 1984, pp. 49-69.

2. Rosenfeld, M.S., and Gause, L.W., in Fatigue of Fibrous Composite Materials, ASTM STP-723, American Society for Testing and Materials, Philadelphia, 1981, pp. 174-196.

3. Konishi, D.Y., and Johnston, W.R., in Composite Materials: Testing and Design (Fifth Conference), ASTM STP-674, S.W. Tsai, Ed., American Society for Testing and Materials, Philadelphia, 1979, pp. 597-619.

4. Chai, H., Knauss, W.G., And Babcock, C.D., Experimental Mechanics, Vol. 23, No. 3, Sept. 1983, pp. 329-337.

5. Chai, H., Babcock, C.D., and Knauss, W.G., International Journal of Solids and Structures, Vol. 17, No. 11, 1981, pp. 1069-1083.

6. Whitcomb, J.D., in Effects of Defects in Composite Materials, ASTM STP-836, American Society for Testing and Materials, Philadelphia, 1984, pp. 175-193.

7. Whitcomb, J.D., Journal of Composite Materials, Vol. 15, No. 5, Sept. 1981, pp. 403-426.

8. Kapania, R.K., and Wolfe, D.R., in 28th AIAA/ASME/ASCE/AHS Structures, Structural Dynamics, and Materials Conference, American Institute of Aeronautics and Astronautics, New York, 1987, pp. 766-775.

9. Grady, J.E., and Sun, C.T., in Composite Materials: Fatigue and Fracture, ASTM STP-907, H.T. Hahn, Ed., American Society for Testing and Materials, Philadelphia, 1986, pp. 5-31.

10. Simitses, G.J., and Sallam, S., "Delamination Buckling and Growth of Flat Composite Structural Elements," AFOSR-85-1067TR, Sept. 1984. (Avail. NTIS, AD-A162370).

11. MacNeal, R.H., Ed. The NASTRAN Theoretical Manual, (Level 15.5), MacNeal-Schwendler Corp., 1972.

12. Whitcomb, J.D., and Shivakumar, K.N., "Strain-Energy Release Rate Analysis of a Laminate with a Postbuckled Delamination," NASA TM-89091, National Aeronautics and Space Administration, Washington, D.C., 1987.

Address	Module	Function
5	LABEL	Begin buckling analysis
9	MATMOD	Strip displacement vector {δ} from transient solution matrix at each time step
10	EMG	Generate element stress stiffening matrices, $[k_\sigma]$
11	EMA	Assemble global stress stiffening matrix, $[K_\sigma]$
12-22		Eliminate boundary conditions; reduce $[K_\sigma]$
24	ADD	Multiply $[K_\sigma]$ by (-1.0)
25	DPD	Red eigenvalue extraction data from input
27	READ	Eigenvalue extraction: solve $\left[[K] + \lambda[K_\sigma]\right] \{\phi\} = 0$ for eigenvalues and eigenvectors
29	OFP	Format and print eigenvalues
30	SDR1	Recover dependent degrees of freedom for eigenvectors
31	SDR2	Prepare eigenvectors for output
32	OFP	Format and print eigenvectors
37	REPT	Return to address 5

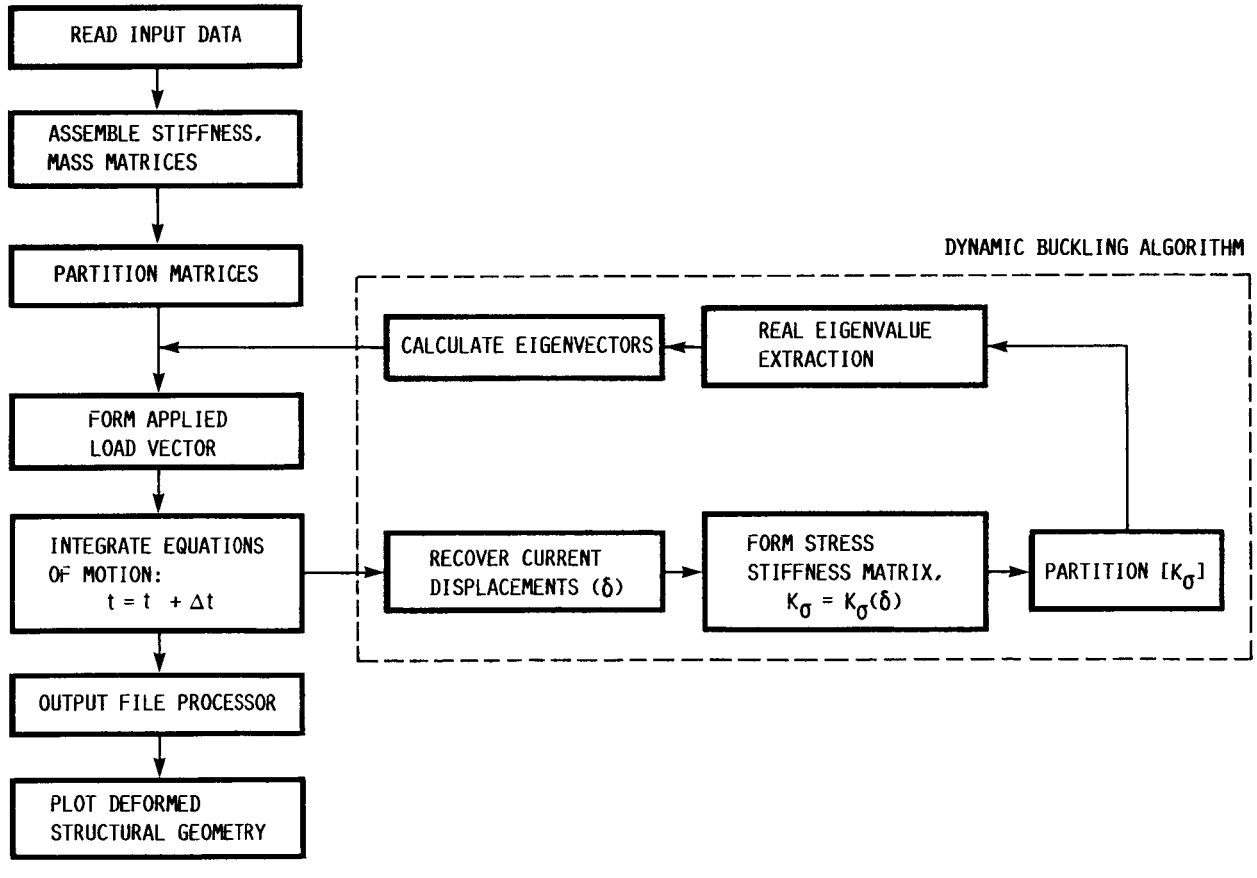

FIGURE 1. - DYNAMIC BUCKLING ANALYSIS FLOW CHART.

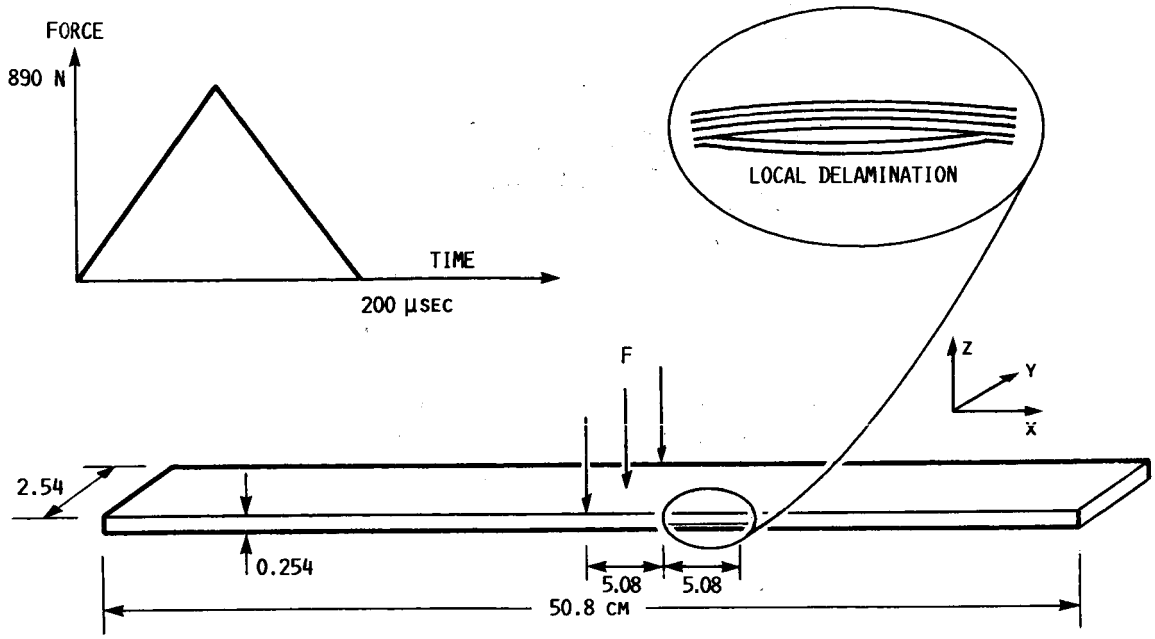

FIGURE 2. - IMPACT SPECIMEN GEOMETRY AND LOADING.

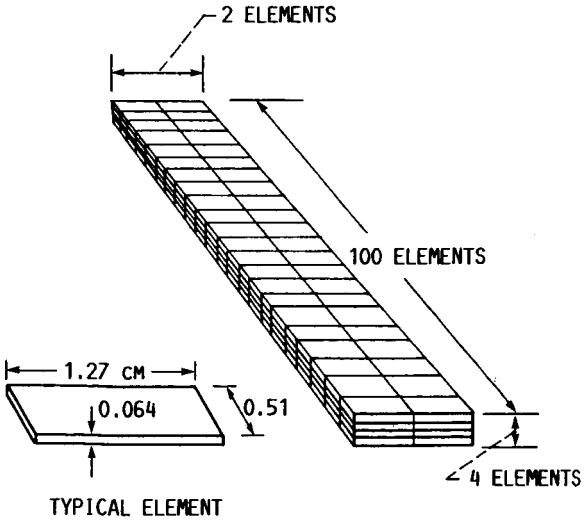

FIGURE 3. - FINITE ELEMENT MODEL OF IMPACT SPECIMEN.

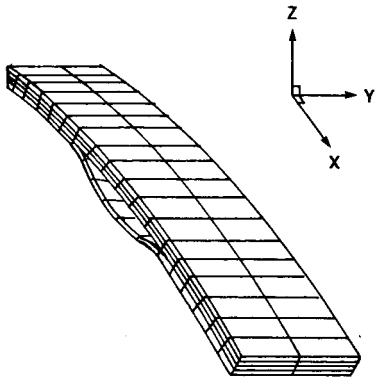

FIGURE 4. - IMPACT SPECIMEN AND BUCKLED SUBLAMINATE.

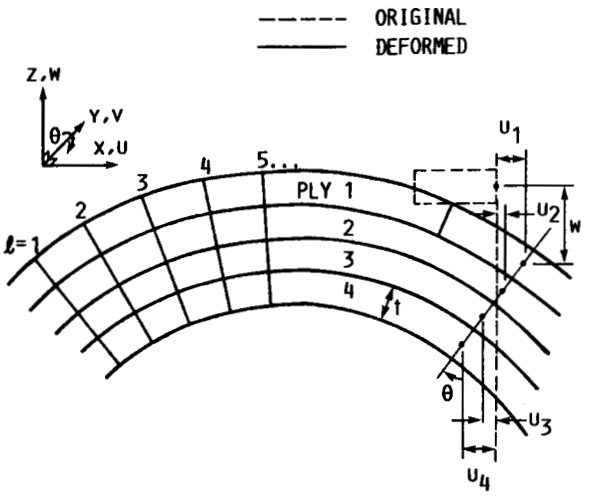

CONSTRAINTS IMPOSED AT EACH LONGITUDINAL STATION 'ℓ':

1. UNIFORM ROTATION AT EACH CROSS SECTION

$$\theta_i \equiv \theta \qquad i = 1,2,3,4$$

2. PLANE SECTIONS REMAIN PLANE

$$u_i - u_{i+1} = t\theta \qquad i = 1,2,3$$

3. NO TRANSVERSE STRAIN ($\varepsilon_z = 0$)

$$w_i \equiv w \qquad i = 1,2,3,4$$

FIGURE 5. - EXAGGERATED DEFORMATION OF FINITE ELEMENT MODEL.

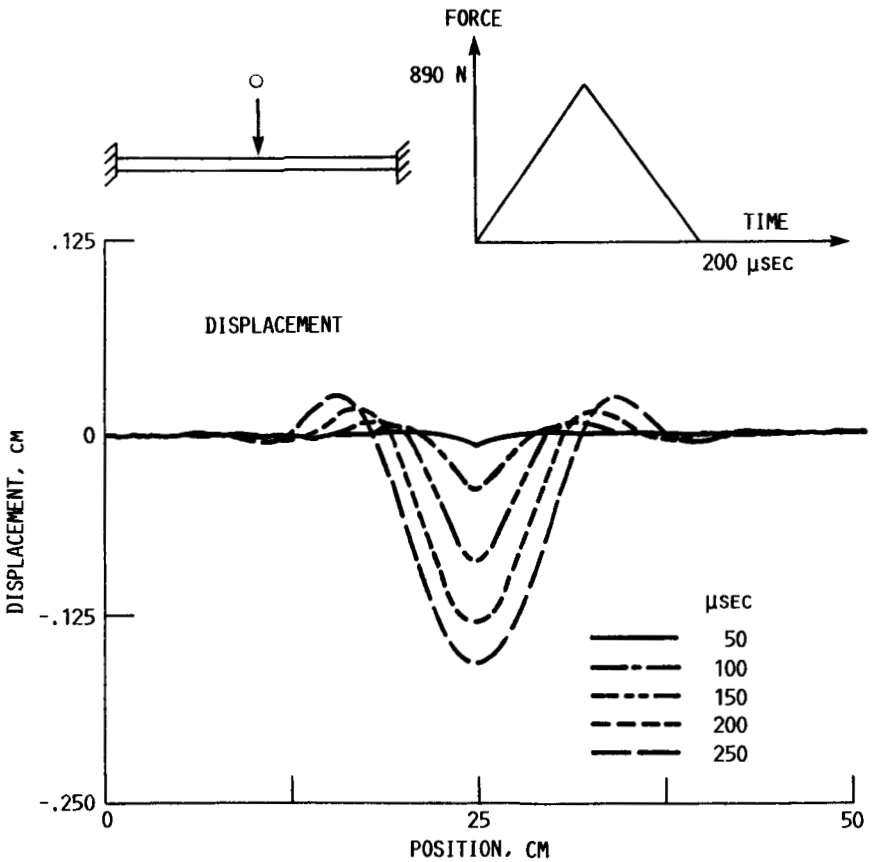

FIGURE 6. - MIDPLANE DISPLACEMENT PROFILES OF IMPACT SPECIMEN DUE TO A CENTRAL IMPACT.

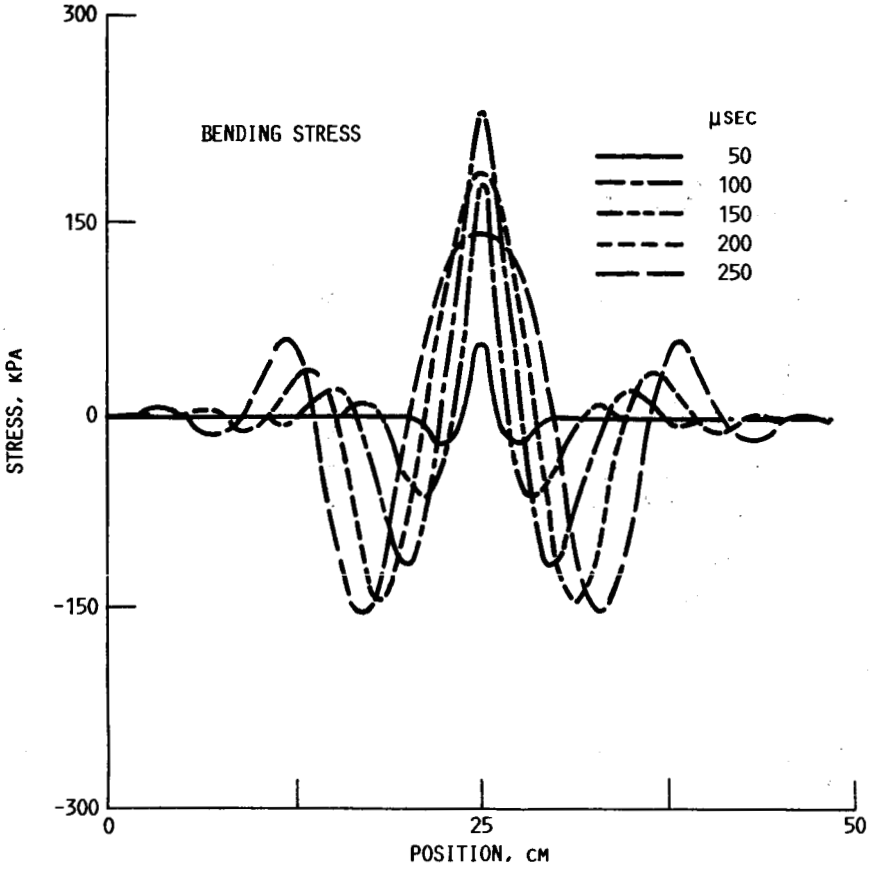

FIGURE 7. - DISTRIBUTION OF MAXIMUM BENDING STRESS IN IMPACT SPECIMEN DUE TO A CENTRAL IMPACT.

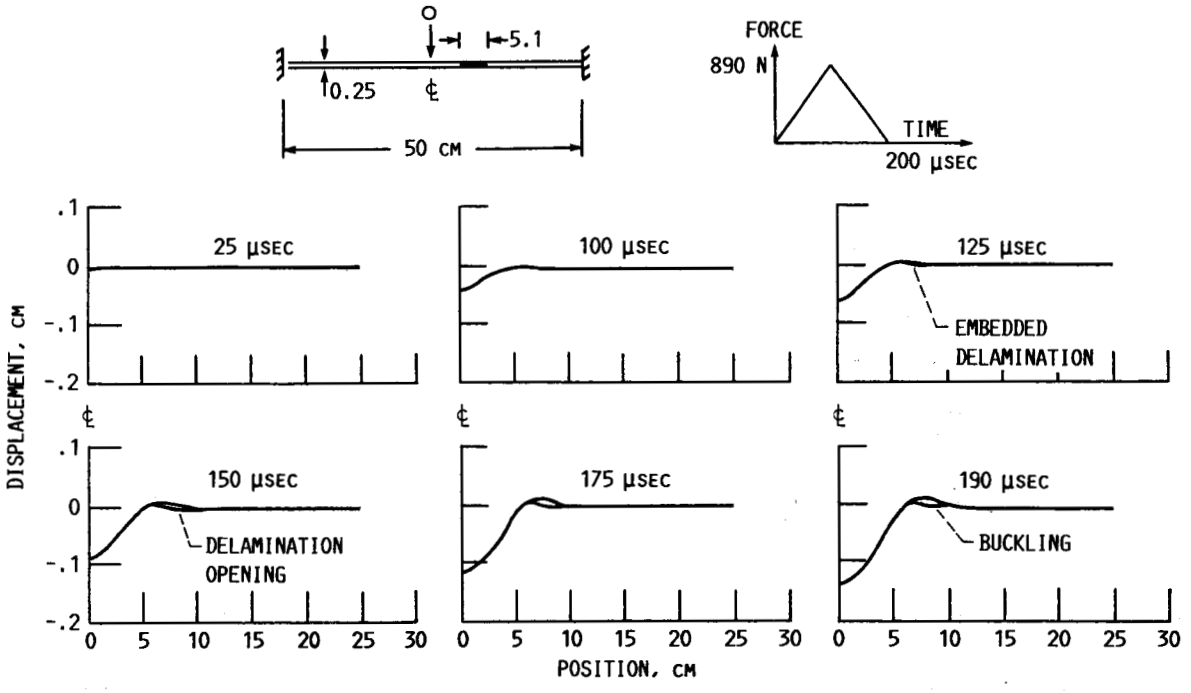

FIGURE 8. - DISPLACEMENT PROFILES OF RIGHT HALF OF IMPACT SPECIMEN WITH INITIAL OFF-MIDPLANE DELAMINATION DUE TO A CENTRAL IMPACT.

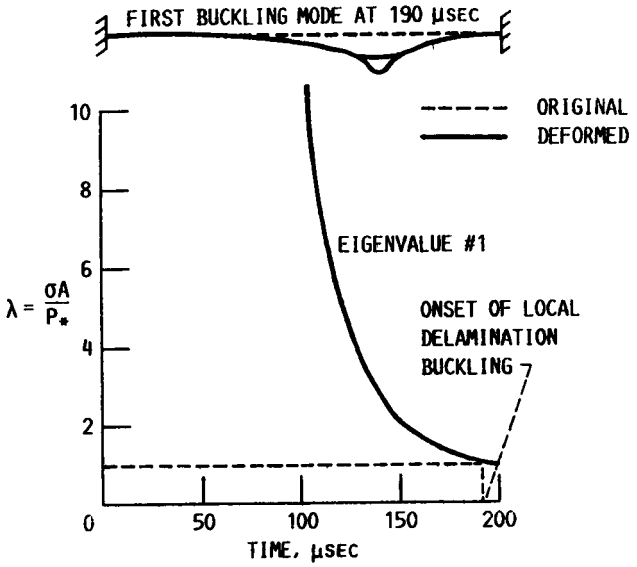

FIGURE 9. - CALCULATION OF DYNAMIC BUCKLING INSTABILITY POINT.

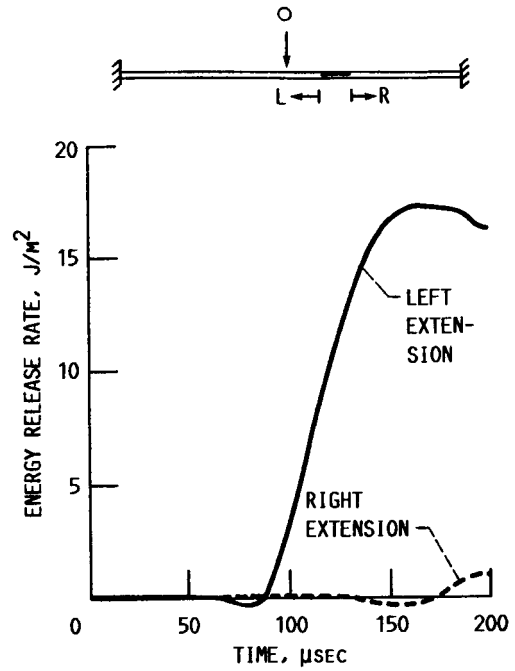

FIGURE 10. - STRAIN ENERGY RELEASE RATES FOR EXTENSION OF ORIGINAL DELAMINATION IN OPPOSITE DIRECTIONS.

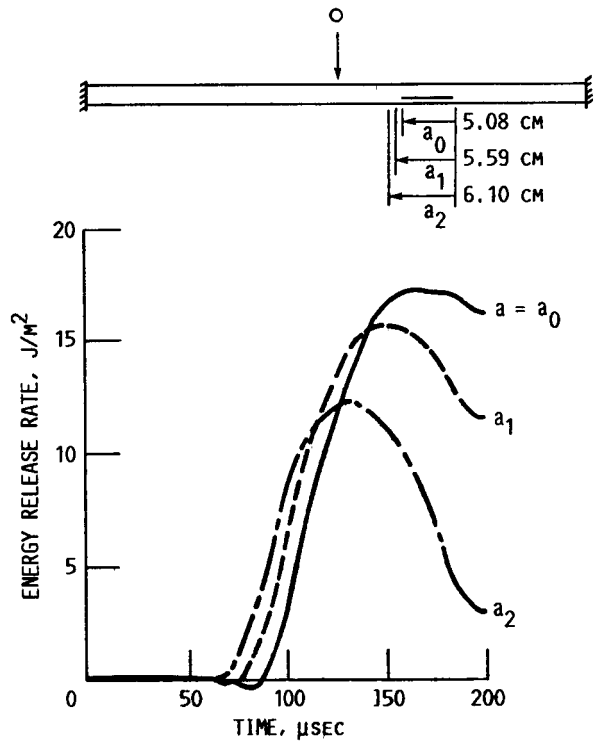

FIGURE 11. - STRAIN ENERGY RELEASE RATES FOR PROGRESSIVE EXTENSION OF ORIGINAL DELAMINATION TOWARD THE POINT OF IMPACT.

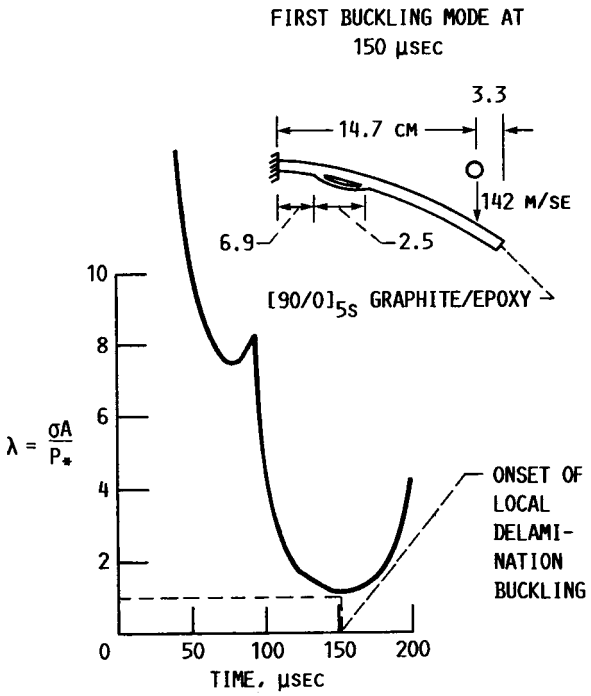

FIGURE 12. - LOWEST BUCKLING EIGENVALUE FOR CANTILEVERED LAMINATE WITH AN INITIAL DELAMINATION.

NASA
National Aeronautics and Space Administration

Report Documentation Page

1. Report No.	2. Government Accession No.	3. Recipient's Catalog No.
NASA TM-100192		

4. Title and Subtitle

Dynamic Delamination Buckling in Composite Laminates Under Impact Loading: Computational Simulation

5. Report Date

6. Performing Organization Code

7. Author(s)

Joseph E. Grady, Christos C. Chamis, and Robert A. Aiello

8. Performing Organization Report No.

E-3779

10. Work Unit No.

505-63-11

9. Performing Organization Name and Address

National Aeronautics and Space Administration
Lewis Research Center
Cleveland, Ohio 44135-3191

11. Contract or Grant No.

13. Type of Report and Period Covered

Technical Memorandum

12. Sponsoring Agency Name and Address

National Aeronautics and Space Administration
Washington, D.C. 20546-0001

14. Sponsoring Agency Code

15. Supplementary Notes

Prepared for the Second Symposium on Composite Materials: Fatigue and Fracture, sponsored by the American Society for Testing and Materials, Cincinnati, Ohio, April 26-30, 1987.

16. Abstract

A unique dynamic delamination buckling and delamination propagation analysis capability has been developed and incorporated into a finite element computer program. This capability consists of: (1) a modification of the direct time integration solution sequence which provides a new analysis algorithm that can be used to predict delamination buckling in a laminate subjected to dynamic loading, and (2) a new method of modeling the composite laminate using plate bending elements and multipoint constraints. This computer program is used to predict both impact induced buckling in composite laminates with initial delaminations and the strain energy release rate due to extension of the delamination. It is shown that delaminations near the outer surface of a laminate are susceptible to local buckling and buckling-induced delamination propagation when the laminate is subjected to transverse impact loading. The capability now exists to predict the time at which the onset of dynamic delamination buckling occurs, the dynamic buckling mode shape, and the dynamic delamination strain energy release rate.

17. Key Words (Suggested by Author(s))	18. Distribution Statement
Composite materials; Delamination; Buckling; Impact; Fracture; Finite elements	Unclassified - Unlimited Subject Category 24

19. Security Classif. (of this report)	20. Security Classif. (of this page)	21. No of pages	22. Price*
Unclassified	Unclassified	13	A02

NASA FORM 1626 OCT 86

*For sale by the National Technical Information Service, Springfield, Virginia 22161